

Short paper

A Proposed Transient Recovery  
Voltage Mitigation Technique For  
Generator-Circuit-Breaker Fed Faults

*In this paper, the generator-circuit-breaker (GenCB) is simulated using ATP-EMTP. The four main stages of the breaker's operating processes are considered, namely; the closed contacts stage, the arc burning stage, the arc extinguishing stage and the opened contacts stage. Therefore, not only the dynamic conductance during current zero are considered but also the effects of arc voltage on the arcing times are included. The simulation is tested in a representative network and the results are compared with IEEE Generator Circuit Breaker standards. Furthermore, a new mitigation technique is introduced to reduce the transient recovery voltage (TRV) and the rate of rise of re-striking voltage (RRRV) during switching period. The results show that the proposed technique successfully reduces both the TRV and RRRV.*

**Keywords:** GenCB, TRV, RRRV, Fed Faults, ATP-EMTP.

## 1. INTRODUCTION

Generator-fed fault currents are subjected to very demanding condition called "Delayed current zeros". This unique characteristic of the fault current comes from the very high X/R (inductive reactance to resistance) ratio of the circuit and the operating conditions of the generator, which can combine to produce a DC component of the fault current exceeding 100%. This means that the asymmetrical fault current peak becomes so high, and its decay is so slow, that the first current zero can be delayed for several cycles [1].

Since circuit breakers rely on current zero crossing in order to interrupt, generator circuit breakers must be able to withstand longer arcing times and greater electrical, thermal and mechanical stresses when interrupting this kind of fault. Different mathematical circuit breaker models exist and are mostly characterized by experimentally measured parameters to describe the dielectric properties of different phenomena which take place in the breaker opening process. At the moment, there is no existing precise universal arc model because of the complexity of the arc physics [2]. On the other hand, most of the models mainly focus on describing the breaker behavior during the current zero periods and ignore the importance of arc voltage. In this paper, the arc voltage is undertaken in the simulation. Furthermore, a proposed technique to suppress TRV and to decrease RRRV is introduced.

## 2. Modeling of the Generator-Circuit-Breaker

The circuit breaker is modeled as a black-box with variable conductance. The value of conductance is determined by a mathematical model, which comprises four sub-stages: a closed breaker stage, an arcing stage, an arc extinguishing stage and an open stage [3-4].

A constant resistance with a value of  $1 \mu$  is used for modeling the closed circuit breaker and constant resistance of  $1 M$  is used for the open circuit breaker model after successful arc extinguishing.

The arcing stage and the extinguishing stage are modeled by using a series connection of a Cassie and Mayer arc model as given in equations (1) and (2) [5-9].

\* Corresponding author: Ebrahim A. Badran, Electrical Engineering Department, Faculty of Engineering, Mansoura University, Egypt, Email: ebadran@mans.edu.eg

1 Electrical Engineering Department, Faculty of Engineering, Mansoura University, Egypt.

2 Electrical Engineering Department, Faculty of Engineering at Shoubra, Benha University, Egypt.

$$\frac{dg_c}{dt} = \frac{1}{\dagger_c} \left( \frac{i^2}{U_c^2 g_c} - g_c \right) \tag{1}$$

$$\frac{dg_m}{dt} = \frac{1}{\dagger_m} \left( \frac{i^2}{p_o} - g_m \right) \tag{2}$$

The total conductance of the arc model during this stage is calculated using equation (3) and is applied in the simulation for the arc extinguishing stage.

$$\frac{1}{g} = \frac{1}{g_c} + \frac{1}{g_m} \tag{3}$$

where;  $i$  is the current through the breaker,  $g_m$  is the conductivity of Mayer’s model part,  $g_c$  is the conductivity of Cassie’s model part,  $\dagger_m$  is the Mayer time constant,  $\dagger_c$  is the Cassie time constant,  $U_c$  the constant voltage for Cassie arc model, and  $p_o$  is the constant power of Mayer arc model.

The four sub-models form a combined contact model. Once the contact receives open signal, each sub-model is activated at the corresponding time.

### 3. Generator Fed Faults

Fig. 1a shows the two key unique fault current conditions encountered by generator circuit breakers [1-2]. ATP-EMTP is used to simulate the generator fed fault at B in Fig. 1a. The simulation of the generator fed fault by using the proposed circuit breaker model is shown in Fig. 1b. There is usually a cable connected between the GenCB and the step up transformer, hence the demonstration circuit comprises a voltage source, a GenCB, a cable and a fault initiated at the end of the cable. The tested circuit breaker parameters are given in Table 1.

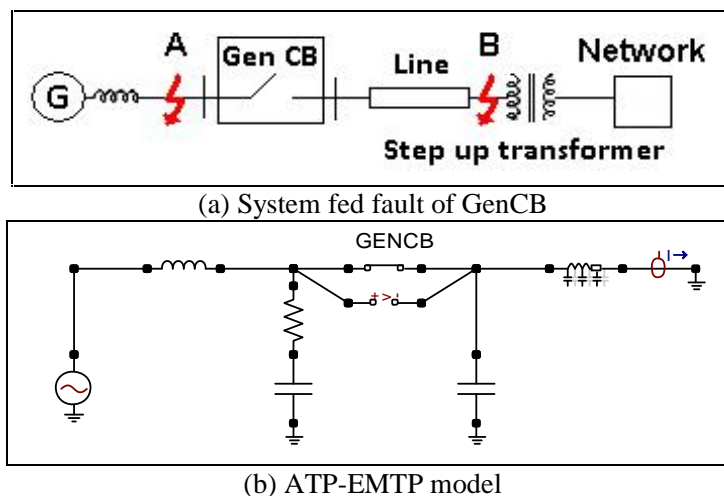


Fig. 1: The Test System

The important ratings must be considered for the TRV are the TRV peak, the time to the TRV peak, and the rate of rise of recovery voltage. The TRV across the circuit breaker contacts is calculated from:

$$V_{TRV} = E_1 \left[ 1 - \cos \left( t / \sqrt{L_t C_t} \right) \right] \tag{4}$$

where  $L_t$  is the total leakage inductance in Henry,  $C_t$  is the total capacitance in Farad,  $t$  is the time in seconds, and  $E_1$  is calculated from:

$$E_1 (kV) = 1.5 \sqrt{2} I \tilde{S} L_t \tag{5}$$

where  $\tilde{S} = 2ff$  and  $I$  is the fault current in kA (rms).

Table 1: Constants of tested circuit breaker model

Constant power of Mayer arc model ( $p_o$ )	8800
Mayer time constant ( $t_m$ )	2.2E-7
Cassie time constant ( $t_c$ )	8E-7
Constant voltage for Cassie arc model ( $U_c$ )	2350

The voltage across the circuit breaker at current interruption of 20 kA short circuit current is shown in Fig. 2. It is noticed that at current zero, the voltage oscillates with a high frequency. After the period of high oscillation the voltage oscillates at 60 Hz, with a value of 20.4 kV and reached from zero to crest value of TRV of 41.801 kV in time of 10.9  $\mu$ s, i.e. the RRRV is 4.511 kV/ $\mu$ s. Following the decay of transient, the voltage oscillates at 60 Hz with 20.4 kV, as shown in Fig. 2.

Fig. 3 shows the voltage across the circuit breaker at current interruption of 60 kA short circuit. It is noticed that the TRV oscillates with lower oscillation than the case of 20 kA short circuit. At current zero the voltage oscillates with high frequency and first TRV peak of oscillation reaches a value of about 40.654 kV in a time of 6.6  $\mu$ s. The RRRV is about 7.2467 kV/ $\mu$ s which is larger than that of the 40 kA case. Following the decay of transient, the voltage oscillates at 60 Hz with 20.4 kV.

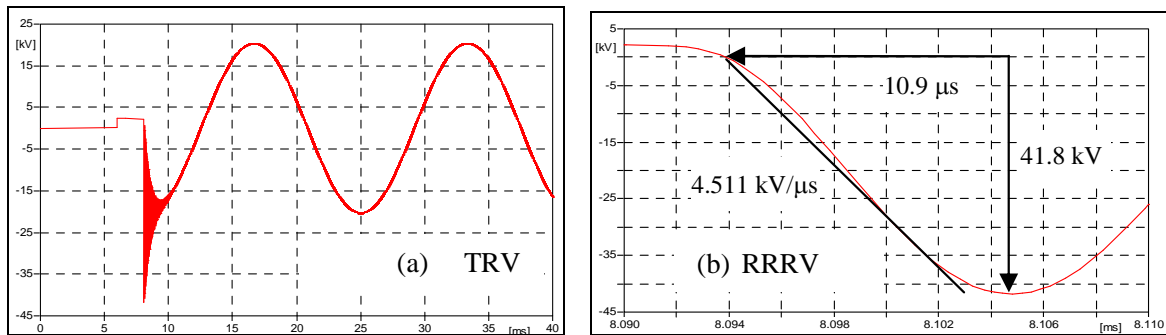


Fig. 2: TRV and RRRV of the 20 KA short-circuit

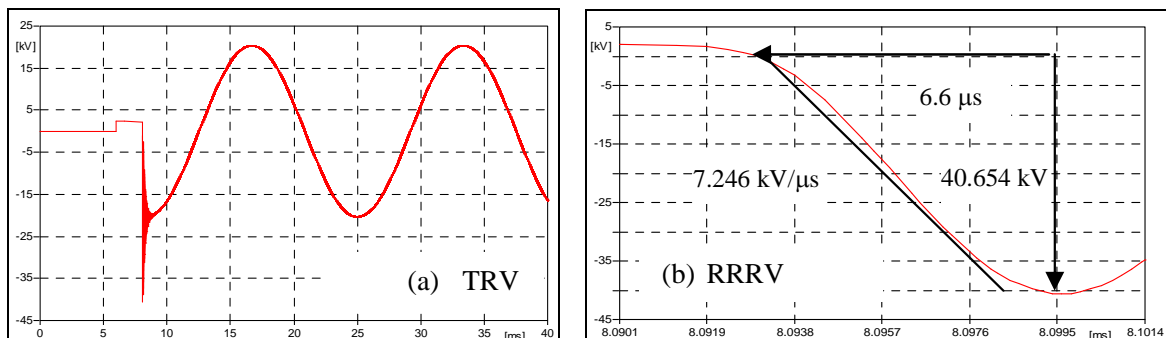


Fig. 3: TRV and RRRV of the 60 KA short-circuit

The voltage across the circuit breaker at current interruption of 80 kA short circuit is shown in Fig. 4. It is noticed that the reignition is happened at first current zero and the interruption of short circuit current is happened at the second current zero. After that the TRV oscillates with high oscillation and the first TRV peak of oscillation reaches the value of about 40.308 kV in a time of 6.4  $\mu$ s. The RRRV is about 7.4 kV/ $\mu$ s. Following the decay of transient, the voltage oscillates at 60 Hz with 20.4 kV. The voltage across the circuit breaker in case of 100 kA and 130 kA short circuit is shown in Fig. 5. It is seen that the circuit breaker fails to interrupt the two short circuit levels.

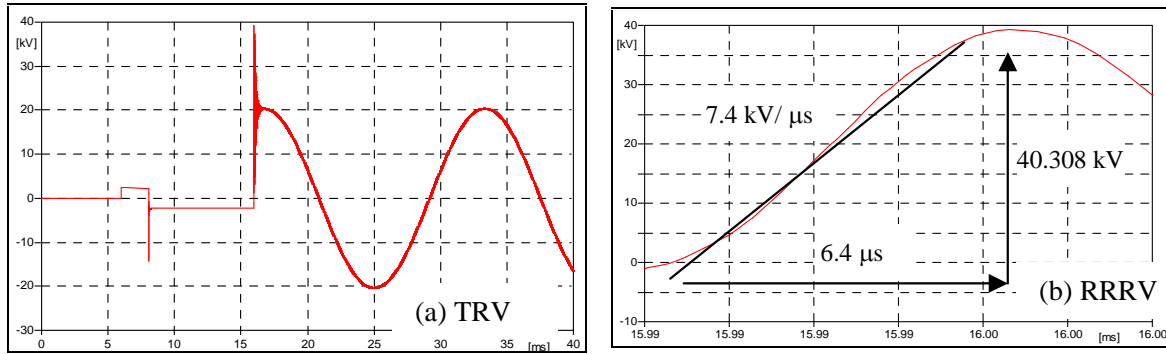


Fig. 4: TRV and RRRV of the 80 KA short-circuit

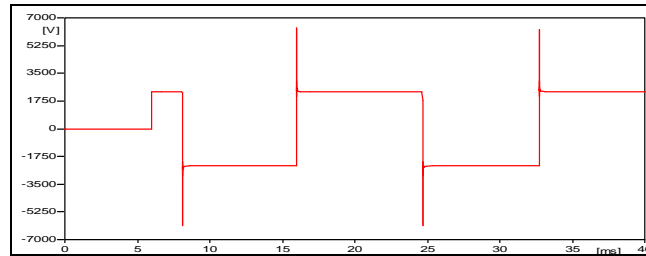


Fig. 5: Voltage across the circuit breaker

Figs. 6 and 7 show the voltage across the circuit breaker in case of 20 kA three phase short circuit current in case of three-phase model. It is noticed that the arcing times of phase A, phase B and phase C are 0.1032 ms, 5.307 ms and 2.6233 ms, respectively. The TRV peaks of phase A, phase B and phase C are 28.608 kV, 24.603 kV and 25.711 kV, respectively. The rate of rise of recovery voltages of phase A, phase B and phase C are 3.17 kV/μs, 4.134 kV/μs and 2.936 kV/μs, respectively. The time to crest of phase A, phase B and phase C are 10.6 μs, 7 μs and 10.3 μs, respectively.

#### 4. TRV Mitigation of GenCB

It is proposed to use capacitor-resistance (C-R) suppressor across the GenCB to suppress the TRV. Fig. 8 shows the voltage across circuit breaker without suppressor and with the proposed C-R suppressor of  $R=30 \Omega$  and  $C=300 \text{ nF}$ . It is noticed that for the waveform without using the suppressor, the TRV and the RRRV are 41.801 kV and 4.5117 kV/μs, respectively. While with using the C-R suppressor of  $R=30 \Omega$  and  $C=300 \text{ nF}$ , the TRV and RRRV are 33.980 kV and 0.6335 kV/μs, respectively. It is also shown that the high frequency oscillation is damped.

Fig. 9 shows the voltage across circuit breaker without and with C-R suppressor of  $R=30 \Omega$ ,  $C=300 \text{ nF}$ , respectively, in case of three-phase model. It is noticed that the first waveform has a high voltage oscillation without using C-R suppressor. The RRRV of phase A, phase B and phase C are 3.175 kV/μs, 4.1340 kV/μs, and 2.9360 kV/μs, respectively, while they are reduced with using C-R suppressor of  $C=300 \text{ nF}$ ,  $R=30 \Omega$  to 0.4445 kV/μs, 0.3616 kV/μs, and 0.4039 kV/μs, respectively. It is also shown that the high frequency oscillation is removed with using the C-R suppressor.

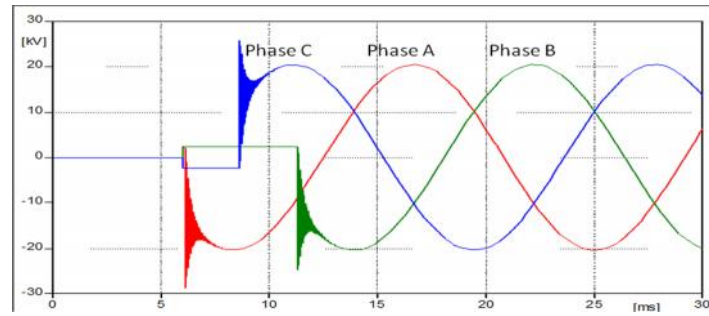


Fig. 6: The voltage across the circuit breaker in case of 20 kA short circuit current for the three-phase model

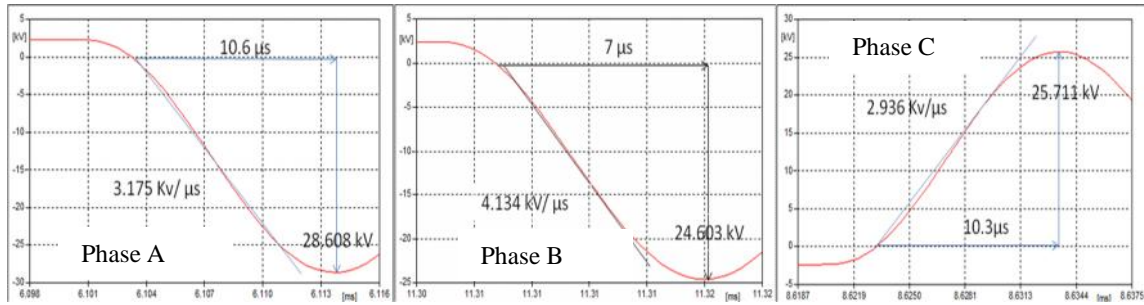


Fig. 7: The crest value of transient recovery voltage and RRRV of 20 KA short circuit for the three-phase model

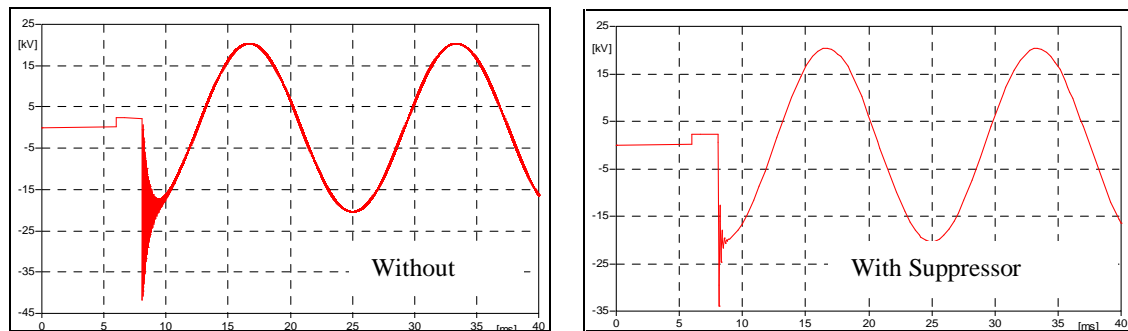


Fig. 8: Voltage across the circuit breaker at 20 kA short circuit without and with C=300 nF and R=30 Ω suppressor

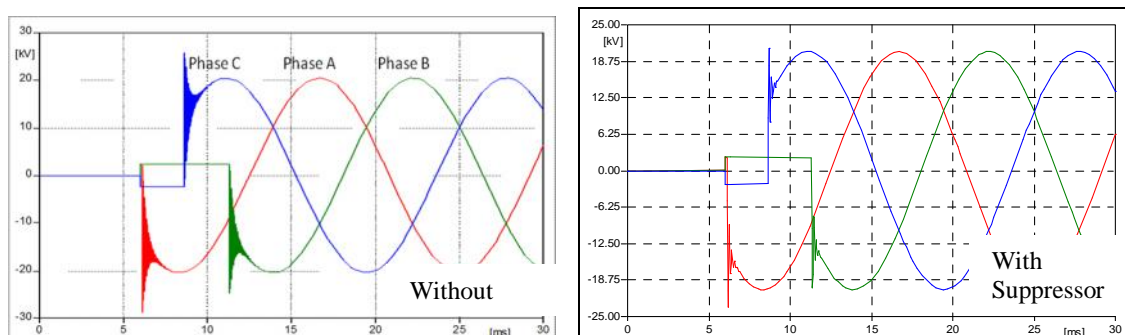


Fig. 9: Voltage across the circuit breaker at 20 kA short circuit without and with C=300 nF and R=30 Ω suppressor in case of three-phase model

Table 2 shows the TRV, RRRV and time to crest of 20 kA short circuit current at C-R suppressor of R=30 Ω and C varies from 40 nF to 300 nF. It is noticed that as the capacitance increases the TRV and RRRV decreases while the time to crest increases.

Fig. 10 shows the TRV versus the capacitance value of the proposed C-R suppressor. It is noticed that as the value of surge capacitance increases the TRV decreases. The TRV

decreased by 5.622 kV when the capacitance increases from 40 nF to 300 nF, at 20 kA short circuit. As the short circuit current increases from 20 kA to 130 kA at capacitance of 40 nF, TRV decreases by 4.198 kV.

Table 2: TRV, RRRV, and the time to crest of TRV at 20 kA in case of C-R suppressors with R=30

Capacitance (nF)	TRV (kV)	RRRV (kV/μs)	Time to crest of TRV (μs)
40	39.512	1.531	25.8
80	37.912	1.282	34.8
120	36.818	1.044	41.5
160	35.978	0.893	47.4
200	35.292	0.791	52.5
240	34.712	0.715	57.1
280	34.209	0.659	61.1
300	33.980	0.634	63.1

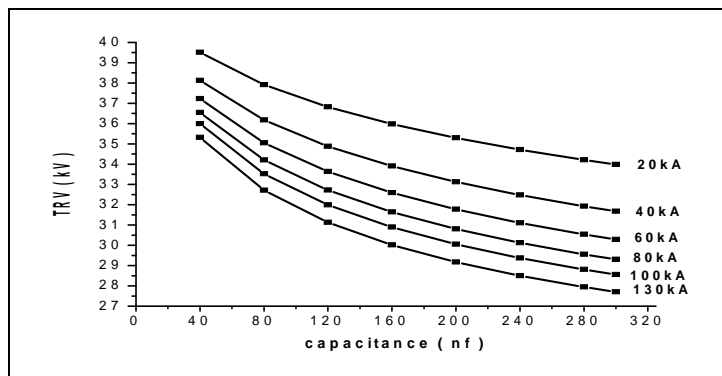


Fig. 10: TRV Vs capacitance of suppressor with R=30 at different short circuit current

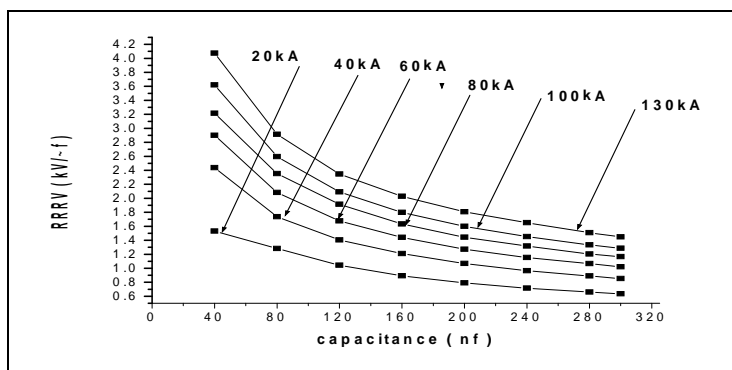


Fig. 11: RRRV Vs capacitance of suppressor with R=30 at different short circuit current

Fig. 11 shows the RRRV versus the capacitance of the proposed C-R suppressor. It can be seen that as the value of capacitance increases the RRRV decreases. When the value of capacitance increases from 40 nF to 300 nF at 20 kA short circuit the RRRV decreases by 0.897 kV/μs. The RRRV increases by 2.542 kV/μs when the short circuit current increases from 20 kA to 130 kA at capacitance of 40 nF.

The change of time to crest with the capacitance values at different short circuit currents is shown in Fig. 12. It is noticed that as the value of the capacitance increases the time to crest increases. Also, it can be found that at a certain value of the capacitance, the time to crest increases as the short circuit current decreases. The time to crest is increased by about 37.3 μs as the surge capacitance increased from 40 nF to 300 nF at 20 kA short circuit current. The time to crest decreases from 25.8 μs to 10.2 μs as the short circuit current increases from 20 kA to 130 kA, at capacitance of 1 μF.

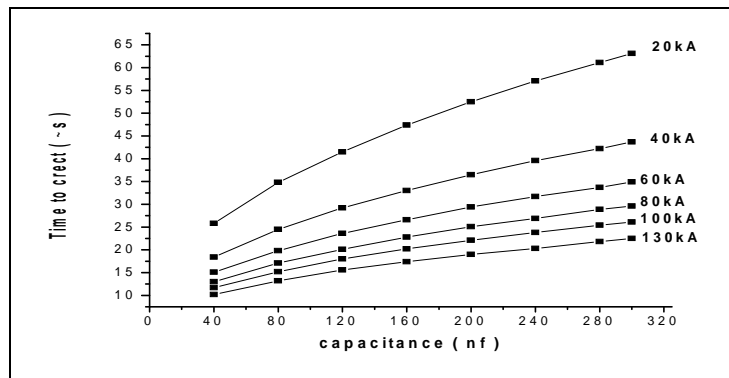


Fig. 12: The time to crest Vs capacitance of suppressor with  $R=30$  at different short circuit current

## 5. Conclusion

The voltage across the GenCB oscillates with a high frequency and reached a high value which can be as high as 2 pu in very small time which can be as low as  $6 \mu s$ . In this paper, the proposed mitigation technique using C-R suppressor effectively reduced both TRV and RRRV. As the capacitance of C-R suppressor increases, the TRV and RRRV are decreased, while the time to crest is increased. At a certain value of capacitance, as the short circuit increases, the TRV and time to crest are decreased while RRRV is increased.

## REFERENCES

- [1] Václav Ježek, Perspective Generator Circuit Breaker, Intensive Programme on Renewable Energy Sources, 107-110, 2010.
- [2] IEEE Standard for AC High-Voltage Generator Circuit Breakers Rated on a Symmetrical Current Basis, IEEE Standard C37.013-1997.
- [3] S. Y. Leung, Laurence A. Snider and Cat S. M. Wong, SF6 Generator Circuit Breaker Modeling, International Conference on Power Systems Transients, IPST'05, Montreal, Canada, 2005.
- [4] P. H. Shavemaker and L. Van Der Sluis, The Arc Model Blokset, 2<sup>nd</sup> IASTED International Conference on Power Engineering Systems, 1310-1315, 2002.
- [5] R. P. P. Smeets and W. A. van der Linden, The Testing SF6 Generator Circuit Breakers, IEEE Transactions on Power Delivery, 13(4), 1188-1193, 1998.
- [6] Grega Bizak, Peter Zunko and Dusan Povh, Combined Model of SF6 Circuit Breaker for Use in Digital Simulation Programs, Transactions on Power Delivery, 19(1), 174-180, 2004.
- [7] G. Ala and M. Inzerillo, An Improved Circuit Breaker Model in Models Language for ATP-EMTP, International Conference on power Systems Transient, IPST'99, 493-498, 1999.
- [8] R. P. P. Smeets and L.H. Paske, Testing of SF6-and Vacuum Generator Circuit breakers, International Conference on Electric Power equipment-Switching Technology, 146 -150, 2011.
- [9] A. Borghetti, F. Napolitano, C.A. Nucci, M. Paolone, M. Sultan, N. Tripaldi, Transient Recovery Voltages in Vacuum Circuit Breakers Generated by the Interruption of Inrush Currents of Large Motors, International Conference on power Systems Transient, (IPST2011) in Delft, the Netherlands June 14-17, 2011.